small oscillation region and the spoke region may show how to extend quasi-linear calculations to apply in the latter.

References

[1] Malliaris, A. C., "Investigation of Acceleration Mechanisms in MPD Accelerators," ARL 68-0078, April 1968, U. S. Air Force Aerospace Research Lab., Wright-Patterson Air Force Base, Ohio.

[2] Allario, F., Jarrett, O., Jr., and Hess, R. V., "Onset of Rotating Disturbances in the Interelectrode Region and Exhaust Jet of an MPD Arc," AIAA Paper 69-232, New York, 1969.

[3] Larson, A. V., "Experiments on Magnetoplasmadynamic Engines with Rotating Current Distributions," NASA CR-66803, June 1969, General Dynamics/Convair, San Diego, Calif.

[4] Esker, D. W., Kroutil, J. C., and Checkley, R. J., "Radiation Cooled MPD Arc Thruster," MDC-H296, NASA-CR-72557, July 1969, McDonnell-Douglas Co., St. Louis, Mo.

[5] Larson, A. V., "Experiments on Current Rotations in an MPD Engine," *AIAA Journal*, Vol. 6, No. 6, June 1968, pp. 1001–1006.

[6] Smith, J. M., "Electrothermal Instability—An Explanation of the MPD Arc Thruster Rotating Spoke Phenomenon," AIAA Paper 69-231, New York, 1969.

[7] Hassan, H. A. and Thompson, C. C., "Onset of Instabilities in Coaxial Hall Current Accelerators," *AIAA Journal*, Vol. 7, No. 12, Dec. 1969, pp. 2300–2304.

Note on an Approximate Method for Computing Nonconservative Generalized Forces on Finitely Deformed Finite Elements

J. T. Oden*

Research Institute, The University of Alabama, Huntsville, Ala.

Introduction

In the analysis of finite deformations of deformable bodies by the finite-element method, surface tractions acting on material surfaces in the deformed body are replaced by consistent generalized forces which are concentrated at nodal points on the element boundaries. Typically, the character of these generalized forces is determined on the basis of invariance of the potential energy of the external forces and independence of path of the deformation process, a procedure which tacitly assumes that the forces are conservative. In practical applications, however, the applied forces are rarely conservative. Even in the case of relatively simple loadings (e.g., uniform external pressures), the net generalized forces are not conservative, and in order to account for their variation in magnitude as the body deforms they must be expressed as functions of the displacement gradients at the element boundaries.[1–3] Unfortunately, when correct expressions for consistent nonconservative generalized forces on finitely deformed elements are obtained, they often appear as extremely complicated functions of the nodal displacements. This complexity possibly explains why such forces have rarely been used in finite-element analyses of geometrically nonlinear problems.

In this Note, a relatively simple approximate technique is discussed which leads to simple formulas for nonconservative generalized nodal forces on finitely deformed finite elements. Special cases appropriate for normal pressures are also cited.

Received February 2, 1970; revision received by August 3, 1970. The support of this work by the U. S. Air Force Office of Scientific Research under Contract F44620-69-C-0124 is gratefully acknowledged.

* Professor of Engineering Mechanics. Member AIAA.

Nonconservative Generalized Forces

Consider a discrete model of an arbitrary continuous body which consists of a collection of finite elements connected together at various nodal points. When the body is in a reference configuration C_0, we establish a system of material coordinates x^i, $i = 1$–3, which, for simplicity, are assumed to be rectangular Cartesian, and a corresponding system of orthonormal base vectors i_i. A typical finite element e with N_e nodal points is isolated from the collection, the volume, surface area, and mass density of which are denoted $v_{0(e)}$, $A_{0(e)}$, and ρ_0 while in C_0. Following the usual finite-element procedure, the local displacement field $u_i(\mathbf{x},t)$ over e at time t is approximated by

$$u_i(\bar{x},t) = \psi_N(\mathbf{x})u_i^N \tag{1}$$

where N is summed from 1 to N_e, $\psi_N(\mathbf{x})$ are local interpolation functions, and $u_i^N = u_i^N(t)$ are the components of displacement at node N of the element. With the aid of Eq. (1), all other kinematical quantities can be determined. It is not difficult to show that the components of generalized force at node N are

$$p_{Ni} = \int_{v_{0(e)}} \rho_0 \hat{F}_i \psi_N dv_0 + \int_{A_{0(e)}} \hat{S}_0{}^j(\delta_{ji} + \psi_{M,j}u_i^M)\psi_N dA_0 \tag{2}$$

where $\hat{F}_i$ are components of body force and $\hat{S}_0{}^j$ are components of surface tractions referred to the convected coordinate lines x^i in the deformed body.

The contribution of body forces to p_{Ni} of Eq. (2) present no special problems since the components $\hat{F}_i(\mathbf{x},t)$ are assumed to be prescribed for all $\mathbf{x}$ and t. The surface integral, however, is generally a complicated function of u_i^N. For example, in the case in which the material surface of a finite element is subjected to a normal traction $q = q(\mathbf{x},t)$,

$$\hat{S}^j = qG^{1/2}G^{jk}\hat{n}_k \tag{3}$$

where G^{jk} is the inverse of $G_{ij} = (\delta_{im} + \psi_{M,i}u_m^M)(\delta_{jm} + \psi_{N,j}u_m^N)$, $G = \det G_{ij}$, and $\hat{n}_k$ are the components of a unit vector normal to the undeformed area A_0.

Approximate Forms

Since the generalized nodal forces are quite complicated functions of the nodal displacements, it is natural to seek simplified approximations of these forces. We shall describe one rather general method of approximation which amounts to representing the deformed surface area of an arbitrary finite element by a collection of flat triangular or quadrilateral elements over which the loading is assumed to be uniform.

Consider the surface of an arbitrary type of finite element, as shown in Fig. 1, which undergoes large displacements and distortions due to a general system of applied surface tractions. We ignore body forces here since they are adequately accounted for by Eq. (2). Regardless of the actual form of the local displacement field $u_i = \psi_N u_i^N$, we represent the deformed material surface by a collection of flat elements, generally triangular in shape, the nodal points of which are coincident with those of the original material surface of the element. The applied surface tractions per unit surface area are assumed to be uniform over each flat element. Ideally, if the element is sufficiently small the network of subelements can provide a close approximation to rather general applied loads.

Confining our attention to a typical flat triangular subelement of area a, let $\bar{n}$, $\bar{e}_1$, and $\bar{e}_2$ denote an orthonormal triad of

vectors, $\bar{n}$ being normal to a in the deformed element. The total applied force on a can then be written in the form

$$\bar{S} = a(q_0\bar{n} + s_1\bar{e}_1 + s_2\bar{e}_2) \tag{4}$$

where q_0, s_1, and s_2 are prescribed uniform normal and tangential components of surface force per unit deformed area a. Suppose that the triangular surface on which $\bar{S}$ is applied passes through nodes 1, 2, and 3 of the deformed surface of the element. If $\bar{R}^N = \bar{r}^N + \bar{u}^N = (x_i{}^N + u_i{}^N)\bar{i}_i$ $(i, N = 1\text{–}3)$ denotes position vectors drawn from the reference configuration to the displaced positions of nodes 1, 2, 3, then the sides of the triangle are formed by the two vectors $\bar{A} = \bar{R}^2 - \bar{R}^1$ and $\bar{B} = \bar{R}^3 - \bar{R}^1$. The surface area is then given by

$$a = \tfrac{1}{2}|\bar{A} \times \bar{B}| = \tfrac{1}{2}(A_iA_iB_jB_j - A_iB_iA_jB_j)^{1/2} \tag{5}$$

while the unit normal $\bar{n}$ is

$$\bar{n} = (1/2a)\bar{A} \times \bar{B} = 1/2a(\epsilon^{ijk}A_iB_j\bar{i}_k) \tag{6}$$

If, for example, we set $\bar{e}_1 = \bar{A}/|\bar{A}| = \bar{A}/A_iA_i{}^{1/2}$, then $\bar{e}_2 = \bar{e}_1 \times \bar{n} = [(\bar{A}\cdot\bar{B})\bar{e}_1 - |\bar{A}|\bar{B}]/2a$ and Eq. (4) becomes

$$\bar{S} = \tfrac{1}{2}\,[q_0\bar{A} \times \bar{B} + 1/|\bar{A}|\,(2aS_1 + \cdot\bar{A}\bar{B}S_2)\bar{A} - S_2|\bar{A}|\bar{B}] \tag{7}$$

The associated generalized nodal forces $\bar{p}_N$ can be obtained by simply distributing $\bar{S}$ equally at each node; i.e., $\bar{p}_N = 1/3\bar{S}$, $N = 1, 2, 3$. Alternately, we can write $\bar{p}_N = \bar{S}m_N{}^{(a)}$ where $m_N{}^{(a)} = \int_a(a_N + b_{Ni}x^i)da$. Since the first alternative is generally more straightforward, we choose to write here for all N, $N = 1, 2, 3$,

$$\begin{aligned}\hat{p}_{Nk} = \tfrac{1}{6}\{&q_0\epsilon_{ijk}(x_i{}^2 + u_i{}^2 - x_i{}^1 - u_i{}^1)(x_j{}^3 + u_j{}^3 - \\ &x_j{}^1 - u_j{}^1) + 1/|\bar{A}||\bar{B}|[2aS_1 + S_2(x_i{}^2 + \\ &u_i{}^2 + x_i{}^1 - u_i{}^1)(x_i{}^3 + u_i{}^3 - x_i{}^1 + u_i{}^1)] \times \\ &(x_k{}^2 + u_k{}^2 - x_k{}^1 - u_k{}^1) - S_2[x_r{}^2 + u_r{}^2 - \\ &x_r{}^1 - u_r{}^1)(x_r{}^2 + u_r{}^2 - x_r{}^1 - u_r{}^1)]^{1/2} \times \\ &(x_k{}^3 + u_k{}^3 - x_k{}^1 - u_k{}^1)\}\end{aligned} \tag{8}$$

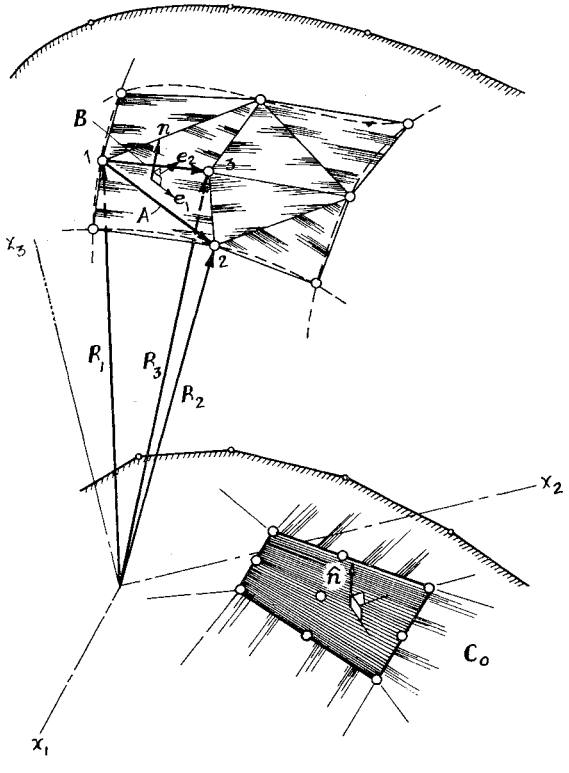

Fig. 1 Approximation of deformed element surface.

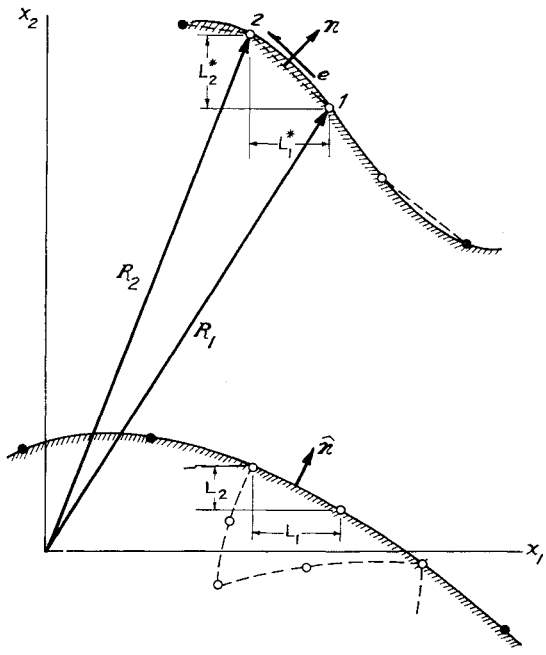

Fig. 2 Approximation of deformed boundary of two-dimensional body.

We note that it may not always be possible or convenient to use the definition of $\bar{e}_1$ given previously; depending upon the nature of the applied loading, different choices of $\bar{e}_1$ may be desirable for different cases. In fact, the base vectors $\bar{e}_1$ and $\bar{e}_2$ in the plane of a need not be orthogonal, and we may simply take $\bar{e}_1 = \bar{A}/|\bar{A}|$ and $\bar{e}_2 = \bar{B}/|\bar{B}|$. Then Eq. (8) reduces to

$$\begin{aligned}\hat{p}_{Nk} = \tfrac{1}{6}\{&q_0\epsilon_{ijk}(x_i{}^2 + u_i{}^2 - x_i{}^1 - u_i{}^1)(x_j{}^3 + \\ &u_j{}^3 - x_j{}^1 - u_j{}^1) + aS_1{}^*(x_k{}^2 + u_k{}^2 - x_k{}^1 - \\ &u_k{}^1)/|\bar{A}| + aS_2{}^*(x_k{}^3 + u_k{}^3 - x_k{}^1 - u_k{}^1)/|\bar{B}|\}\end{aligned} \tag{9}$$

wherein $S_i{}^*$ are the components of $\bar{S}/a$ in the directions of $\bar{e}_i$.

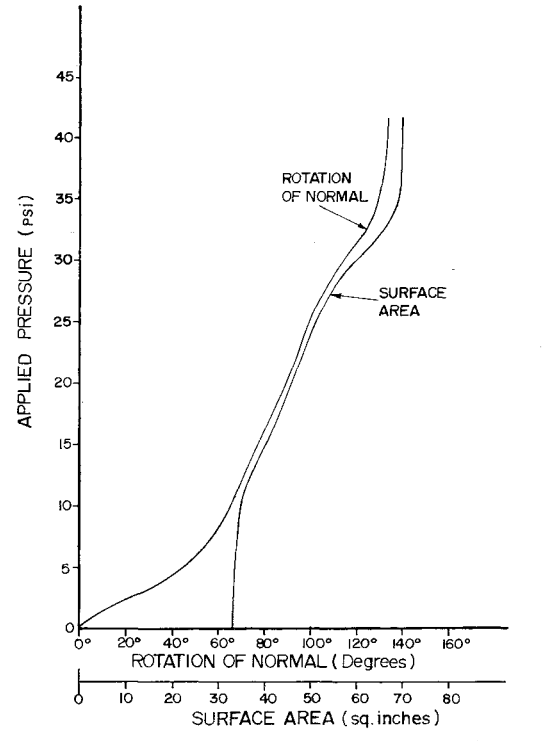

Fig. 3 Variation in orientation and area of a boundary element subjected to increasing external pressure.

The important special case of a uniform normal force $\bar{S} = q_0\bar{an}$ is obtained by equating S_1^* and S_2^* to zero in Eq. (9).

In the case of two-dimensional problems, we may employ essentially the same procedure described above; i.e., a curved boundary in the deformed body is replaced by a collection of straight line segments, as indicated in Fig. 2. In this case, if $\bar{S}$ represents a uniform applied surface traction per unit length and $\bar{n}$ and $\bar{e}$ are unit vectors normal and tangent to the deformed surface,

$$\bar{S} = L^*(q_0\bar{n} + S\bar{e}) \tag{10}$$

where q_0 and S are normal and tangential tractions per unit length, and

$$L^* = |\bar{R}^2 - \bar{R}^1| = [(x_\alpha{}^2 + u_\alpha{}^2 - x_\alpha{}^1 - u_\alpha{}^1) \times (x_\alpha{}^2 + u_\alpha{}^2 - x_\alpha{}^1 - u_\alpha{}^1)]^{1/2} \tag{11}$$

$\alpha = 1, 2$. It is easily verified that

$$\bar{n} = 1/L^*(L_2{}^*\bar{i}_1 + L_1{}^*\bar{i}_2) \tag{12}$$

$$\bar{e} = -1/L^*(L_1{}^*\bar{i}_1 - L_2{}^*\bar{i}_2) \tag{13}$$

where $L_i{}^* = L_1 + u_1{}^2 - u_1{}^1$ and $L_2{}^* = L_2 + u_2{}^2 - u_2{}^1$. Here $L_1 = x_1{}^2 - x_1{}^1$, $L_2 = x_2{}^2 - x_2{}^1$ are the projections of the line drawn from node 1–2 on the x_1 and x_2 axes in the undeformed element. Then the associated generalized forces are simply

$$\hat{p}_{Ni} = \tfrac{1}{2}[q_0(L_2 + u_2{}^2 - u_2{}^1) - S(L_1 + u_1{}^2 - u_1{}^1)]$$
$$\hat{p}_{N2} = \tfrac{1}{2}[q_0(L_1 + u_1{}^2 - u_1{}^1) + S(L_2 + u_2{}^2 - u_2{}^1)] \tag{14}$$

for all N, $N = 1, 2$. In the special case of purely normal loading ($S = 0$), the forces $\hat{p}_{N\alpha}$ of Eq. (14) reduce to $(-1)^\alpha\epsilon_{\alpha\beta}q_0L_\beta{}^*/2$, as given in Ref. 3, wherein α, $\beta = 1, 2$, and $\epsilon_{\alpha\beta}$ being the two-dimensional permutation symbol.

Sample Calculations

We cite briefly the results of applying the approximate equations for generalized forces to a representative problem involving finite deformations. The problem considered is the inflation of an initially flat, thick, simply supported, rubber circular plate, 15 in. in diameter and 0.5 in. thick, subjected to a steadily increasing uniform internal pressure. The loading surface of the plate was idealized using 10 finite elements over which the displacement fields are assumed to be quadratic. Solutions obtained using the exact equations for generalized forces were compared with approximate forces computed by idealizing the loading surface with 20 flat triangular elements. The maximum deviation was less than one %. To emphasize the importance of accounting for the effects of deformation of the boundary elements in computing generalized forces in finitely deformed structures, the variation the orientation of a typical boundary element and its cross-sectional area with internal pressure is indicated in Fig. 3. Clearly, the effects of finite distortion of the loading surface may be equally as important as the rotation of the element.

References

[1] Oden, J. T. and Sato, T., "Finite Strains and Displacements of Elastic Membranes by the Finite Element Method," *International Journal of Solids and Structures*, Vol. 3, 1967, pp. 471–488.

[2] Oden, J. T. and Kubitza, W. K., "Numerical Analysis of Nonlinear Pneumatic Structures," *Proceedings of the IASS Colloquium on Pneumatic Structures*, Stuttgart, Germany, 1967.

[3] Oden, J. T. and Key, J., "Numerical Analysis of Finite Axisymmetric Deformations of Incompressible Elastic Solids of Revolution," *International Journal of Solids and Structures*, Vol. 6, 1970, pp. 497–518.

Film Cooling Effectiveness in Hypersonic Turbulent Flow

Aubrey M. Cary Jr.* and Jerry N. Hefner*
NASA Langley Research Center, Hampton, Va.

A paucity of experimental information prevents an accurate evaluation of film cooling as an active system for hypersonic flight vehicles.[1] Available experimental data (mainly for subsonic mainstream flow) when extended to hypersonic speeds indicated that film cooling will not be competitive with other active cooling systems[1]; however, recent investigations[2,3] at Mach 6 show significantly greater effectiveness for film cooling in high-speed turbulent flow than in low-speed flow (see Ref. 2 for a summary of low-speed results). The present Note reports accurate measurements of surface equilibrium temperature downstream of a rearward-facing, two-dimensional slot with tangential mass (air) injection into a thick, hypersonic turbulent-boundary layer.

An insulated flat-plate model with end plates, shown in Fig. 1, was mounted parallel with the tunnel wall of the Langley 20-in. Mach 6 wind tunnel and alined with the bottom lip of the slot. Surface temperatures were measured by flush mounted thermocouples located along the centerline of the insulated plate surface. The slot configuration, shown in the insert of Fig. 1, allowed for slot heights (s) of 0.159, 0.476, and 1.114 cm with a constant lip thickness (t) of 0.159 cm. The slot mass flow rate ($\rho_j u_j$) was uniform over a midspan of at least 21 cm and regulated so that the ratio of measured slot mass flow rate to calculated freestream mass flow rate ($\lambda = \rho_j u_j/\rho_\infty u_\infty$) ranged from 0.06 to 1.60; the flow at the throat of the slot was always sonic and the ratio of slot velocity to freestream velocity (u_j/u_∞) was approximately 0.34. The freestream total temperature ($T_{t,\infty}$) and unit Reynolds number per cm (R/cm) were 472°K and 0.241×10^6, respectively. The total temperature of the slot flow ($T_{t,j}$) varied slightly from run to run (278° to 294°K). From previous measurements the tunnel-wall boundary layer over the slot was known turbulent and approximately 5.08-cm thick with a momentum thickness Reynolds number approximately 3.8×10^4. The tunnel-wall temperature to total temperature ratio was approximately 0.70.

Experimental Results

A summary of the equilibrium temperatures measured downstream of the slot is presented in Fig. 2 in a form which correlated similar data in Ref. 2. The equilibrium temperatures are expressed as a film cooling effectiveness parameter ϵ, where

$$\epsilon = T_{t,\infty} - T_{eq}/T_{t,\infty} - T_{t,j}$$

and T_{eq} the equilibrium surface temperature. The effectiveness is correlated with a distance parameter $(x/s)\lambda^{-0.8}$, where x is chordwise distance downstream of the slot. For these data, local surface temperature was considered to be in equilibrium when for a period of at least 100 sec. This temperature changes less than 0.1%. Only the forward portion of the plate surface had in general reached equilibrium temperature in the test times available (≈1000 sec); thus, equilibrium temperatures at large x/s were not obtained. Data are presented for three slot heights and injection flow rates ranging from $\lambda = 0.06$ to $\lambda = 1.6$. The effectiveness parameter correlates in a relatively narrow band with $(x/s)\lambda^{-0.8}$ for the slot mass flow rates and slot heights of this investigation. The best straight line fairing of the data in Fig. 2 for $(x/s)\lambda^{-0.8}$

Received June 5, 1970; revision received August 6, 1970.

* Aerospace Engineer, Applied Fluid Mechanics Section, Aero-Physics Division. Associate AIAA.